Optica Applicata, Vol. XXVIII, No. 2, 1998

Computer-aided variable wavelength Fourier transform polarizing microscopy of birefringent fibers

DARIUSZ LITWIN, ADEL M. SADIK*

Institute of Applied Optics, ul. Kamionkowska 18, 03–805 Warszawa, Poland.

An automatic fringe analysis is used to measure the spectral dispersion of birefringence of cylindrical textile fibers. The approach presented is based on the optical Fourier transform microscopy of birefringent fibers. The pattern of the optical Fourier transform observed in a polarizing microscope is processed automatically to measure the radius of interference dark fringes as a function of light wavelength. This method allows us not only to calculate the interference orders and the spectral dispersion of birefringence of fibers but also to detect their optical and geometrical microdefects. The image is processed with a computer-controlled automatic analysis system. Examples of applying this method to highly oriented fibers are given.

1. Introduction

In recent years, interferometry has widely been employed for non-destructive testing in many fields of engineering. Interferometric methods play an important role in medicine and industry. Interferometric data provide phase information on the objects tested. This information refers to a variety of physical properties and can be extracted using optical methods.

In general, interference system suffers from the spectral dispersion of the refractive index or birefringence which causes the zero-order fringe to be usually coloured in white light when the difference of the mentioned dispersion between the object, its surrounding medium and the interference system is not balanced. Thus, the determination of the interference order in the image of the object under study is the crucial problem of any measuring technique involving interferometry. The variable wavelength interferometry (VAWI method), which has been developed by PLUTA [1]–[5], is one of the most successful approaches. This technique is especially suitable when used jointly with Pluta's double-refracting interference microscope [6].

The aim of the computer-aided approch presented is to use interference images of the optical Fourier transform (OFT) of birefringent fibers to analyze birefringent properties and possible structural and geometrical defects of highly birefringent polymer fibers. For the first time their OFTs were observed by Pluta about 20 years ago [7], [8]. Pluta stated that a cylindrical birefringent textile fiber can produce

* Permanent address: Faculty of Science, University of Mansoura, Nansoura, Egypt.

specific interference pattern in the exit pupil of the standard polarizing microscope outfitted with a subcondenser slit diaphragm. OFT's occur when the birefringent fiber is oriented diagonally between two crossed polarizers and is trans-illuminated by monochromatic light. These patterns bahave as the optical Fourier transforms. PLUTA [8] was the first who used the optical Fourier transform pattern observed in a polarizing microscope to measure the spectral dispersion of the birefringence of polymer textile fibers. That task was performed manually. Pluta used monochromatic light of continuously variable wavelength to change intensity of the center of the interference pattern from maximally bright to dark, and so on. It is important to note that this method not only gives information on birefringence of the fibers but also visualizes any irregularity in the fiber structure in terms of the distortion of the fringes. This technique does not involve any immersion oils, either as it is usually necessary in conventional polarizing microscopy or microinterferometry of highly birefringent textile fibers. The only disadvantage of this method is that it cannot be used for measurements of weak birefringent fiber because the number of the interference sequences is less than 2. The measurement process using the optical Fourier transforms' technique is particularly useful in fully automatic operation due to the invariance of the optical Fourier transforms when the fiber under study translates within the field of view of the polarizing microscope which creates potential industrial applications.

In the paper presented, an automatic image processing technique for analyzing the optical Fourier transform patterns of the birefringent fibers is presented. A new procedure of the VAWI method is applied to determine correctly the interference orders in the image of the object under study. The main idea of this procedure consists in the relation of the radius of the annular dark fringes to the light wavelength λ for each sequence of interference patterns. The number of these sequences depends on the object birefringence. The light wavelength is continuously varied using Lyot tunable birefringent filter. Starting from the long-wavelength region and passing toward the short-wavelength region ($\lambda_s = \lambda_1 > \lambda_2 \gg \ldots \lambda_N$) a flow of the interference pattern and its annular dark fringes of consecutive orders can be observed. To determine interference order in the OFT image of the object the radii of the annular dark fringes should be precisely measured. The measurement of this radius can be done using a digital image processing technique described in detail in Subsect. 2.6.

Having determined the radii of the annular dark fringes and applied the new procedure based on the VAWI method, the interference orders in the OFT image of the object and then the spectral dispersion of the object birefringence can be calculated. This method makes it possible to carry out the experiment over a narrow range of the visible spectrum in order to measure the initial interference order and the birefringence if two or more fringes are visible in the exit pupil which occurs for highly birefringent fibers. Additionally, this method is suitable for quick and precise detection of irregularities of the geometrical shape of the object under study. The spectral dispersion of weak birefringent objects can also be calculated using this method.

2. Theory

2.1. Focusing properties of birefringent fibers

A birefringent fiber surrounded by the air medium and oriented diagonally between crossed polars acts as a bifocal lens (Fig. 1). The focal lengths $f_\perp$ and $f_\parallel$ are defined by [8]

$$f_\perp = \frac{t}{4}\frac{n_\perp}{(n_\perp - 1)}, \quad f_\parallel = \frac{t}{4}\frac{n_\parallel}{(n_\parallel - 1)} \tag{1}$$

where t, $n_\perp$, $n_\parallel$ are the thickness, ordinary and extraordinary refractive indices of the fiber, respectively.

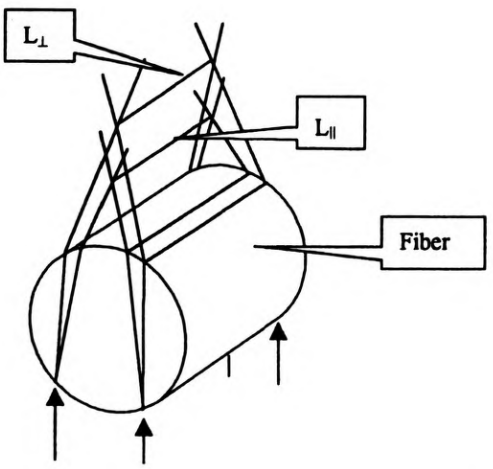

Fig. 1. Birefringent fiber as a bifocal cylindrical lens producing two focal lines

The birefringence B and the optical path difference δ, that are produced by the fiber under study, can be expressed by

$$B = n_\parallel - n_\perp \tag{2}$$

and

$$\delta = tB. \tag{3}$$

2.2. Optical Fourier transform of polymeric textile fibers

About 20 years ago, PLUTA [7], [8] observed that a cylindrical birefringent textile fiber could produce specific interference pattern in the exit pupil of a standard polarizing microscope outfitted with a subcondenser slit diaphragm. A cylindrical birefringent fiber can be regarded as a single-, double-, or multiple-slit source of light depending on its birefringence and the refractive index of its surrounding medium when the fiber is diagonally oriented between crossed polars.

2.2.1. Single-slit OFT

The difference in the focal lengths $f_\perp$ and $f_\parallel$ of a very weak birefringent fiber (shown in Fig. 1) is very slight and two focal lines $L_\parallel$ and $L_\perp$ are hardly resolvable. Therefore the lines can be treated as a one-dimensional Dirac delta function, whose Fourier transform is equal to unity. This means that the wavefront is a plane surface in the Fourier plane of the objective and has the same amplitude over the objective exit pupil provided that the objective does not suffer from any aberration and is not limited. These patterns, however, are not interesting if the measurement point of view is taken into account and are not considered in this paper.

2.2.2. Double-slit OFT

Assuming that a cylindrical birefringent fiber has a significant birefringence, a distance longer than the light wavelength separates its two focal lines. The lines can be considered as two light slits, one of which follows the other. They are mutually coherent across their widths but incoherent along their lengths [8]. Eech pair of coherent points produces spherical wavefronts whose radii of curvature are slightly different. The two wavefronts can interfere with each other and produce an interference pattern with annular/circular fringes observed in the exit pupil of the microscope objective. Any other pair of coherent points gives rise to a separate interference pattern identical with that produced by light wavefronts which are formed from the former two coherent points. These separate interference patterns are mutually incoherent and they occupy the same position in the Fourier plane of the microscope objective. They produce an intense resultant interference pattern of annular symmetry. The advantage of this interference pattern lies in the fact that it does not change its position in the exit pupil of the objective when the cylindrical birefringent fiber is translated transversely or vertically which is the well-known property of the Fourier transformation (see [8], for details). This paper is devoted to measurement techniques based on the analysis of the patterns described above.

2.2.3. Multiple-slit OFT

The focal lengths are actually relatively long when the cylindrical birefringent fiber is immersed in the liquid whose refractive index is n'. Therefore, the optical Fourier transforms of the focal lines are not observed in the exit pupil of the microscope objective. In this case, the cylindrical birefringent fiber behaves as two, three, four, and even more parallel slits of different widths arranged as a line grating in a plane perpendicular to the objective axis. All these slits are localized in or near the object plane of the microscope objective. The width and position of these fringes vary when the light wavelength is changed [8]. In this case, the OFTs have a form of parallel interference fringes similar to Young's interference pattern. These patterns are beyond the scope of this paper.

2.3. Intensity distribution in the Fourier plane using diffraction approach

It is convenient to commence with the assumption that a transparent object (cylindrical birefringent fiber) as shown in Fig. 2 is placed in the plane (u_1, v_1) and

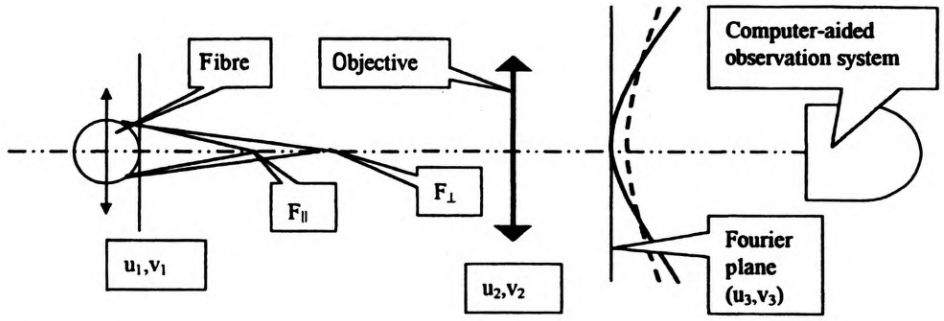

Fig. 2. Fourier transform system

illuminated with a uniform plane wave of unit amplitude. The distribution $\zeta_2(u_2, v_2)$ just before the objective lens is described by the equation

$$\zeta_2(u_2,v_2) = \frac{\exp(iks_1)}{i\lambda \cdot s_1} \int_{-\infty}^{+\infty}\int \zeta_1(u_1,v_1) \exp\left[\frac{ik[(u_2-u_1)^2+(v_2-v_1)^2]}{2s_1}\right] du_1 dv_1 \tag{4}$$

where s_1 is the distance between the planes (u_1, v_1) and (u_2, v_2) and λ is the light wavelength. Substituting

$$g(u,v;s) = \exp\left[\frac{ik(u^2+v^2)}{2s}\right] \tag{5}$$

we arrive at the expression

$$\zeta_2(u_2,v_2) = \frac{\exp(iks_1)}{i\lambda \cdot s_1} g(u_2,v_2;s_1) \int_{-\infty}^{+\infty}\int \zeta_1(u_1,v_1)\, g(u_1,v_1;s_1) \times \exp\left[\frac{ik(u_2u_1+v_2v_1)}{s_1}\right] du_1 dv_1. \tag{6}$$

The resultant distribution $\zeta_3(u_3, v_3)$ (in the exit pupil of the microscope objective) is given by

$$\zeta_3(u_3,v_3) = \frac{\exp(iks_2)}{i\lambda \cdot s_2} g(u_3,v_3;s_2) \int_{-\infty}^{+\infty}\int P(u_2,v_2)\zeta_2(u_2,v_2)\, g(u_2,v_2;-f_{ob})\, g(u_2,v_2;s_2) \times \exp\left[\frac{ik(u_2,u_3+v_2v_3)}{s_2}\right] du_2 dv_2. \tag{7}$$

Making some modifications and assumption that the pupil function P is unity within the range of integration (the lens diameter is large enough), we can rewrite Eq. (7) in the following form [9]:

$$\zeta_3(u_3,v_3)=\frac{1}{i^2\lambda^2\cdot s_1 s_2}g(u_3,v_3;s_2)\iint_{-\infty}^{+\infty}\zeta_1(u_1,v_1)\,g(u_1,v_1;s_1)\iint_{-\infty}^{+\infty}g(u_2,v_2;z)$$
$$\times\exp\left\{-i2\pi\left[u_2\left(\frac{u_1}{\lambda s_1}+\frac{u_3}{\lambda s_2}\right)+v_2\left(\frac{v_1}{\lambda s_1}+\frac{v_3}{\lambda s_2}\right)\right]\right\}\mathrm{d}u_2\,\mathrm{d}v_2\,\mathrm{d}u_1\,\mathrm{d}v_1 \tag{8}$$

where: $\frac{1}{z}=\frac{1}{s_1}+\frac{1}{s_2}-\frac{1}{f_{ob}}$.

If $z=s_1$ and $s_2=f_{ob}$, and the inner integral is calculated, Eq. (8) becomes

$$\zeta_3(u_3,v_3)=\frac{1}{i\lambda f_{ob}}\exp\left[\frac{ik}{2f_{ob}}(u_3^2+v_3^2)\left(1-\frac{s_1}{f_{ob}}\right)\right]\iint_{-\infty}^{+\infty}\zeta_1(u_1,v_1)$$
$$\times\exp\left\{-i2\pi\left[u_1\left(\frac{u_3}{\lambda f_{ob}}\right)+v_1\left(\frac{v_3}{\lambda f_{ob}}\right)\right]\right\}\mathrm{d}u_1\,\mathrm{d}v_1. \tag{9}$$

It is easy to see that it describes the Fourier transform of ζ_1. This formula is applicable to ordinary and extraordinary waves produced by the birefringner fiber, respectively, as follows:

$$\zeta_\perp(u_3,v_3)=\frac{1}{i\lambda f_{ob}}\exp\left[\frac{-ik}{2f_{ob}}(u_3^2+v_3^2)\left(1-\frac{s_1}{f_{ob}}\right)\right]\iint_{-\infty}^{+\infty}\zeta_\perp(u_1,v_1)$$
$$\times\exp\left\{-i2\pi\left[u_1\left(\frac{u_3}{\lambda f_{ob}}\right)+v_1\left(\frac{v_3}{\lambda f_{ob}}\right)\right]\right\}\mathrm{d}u_1\,\mathrm{d}v_1, \tag{10}$$

$$\zeta_\parallel(u_3,v_3)=\frac{1}{i\lambda f_{ob}}\exp\left[\frac{-ik}{2f_{ob}}(u_3^2+v_3^2)\left(1-\frac{s_1}{f_{ob}}\right)\right]\iint_{-\infty}^{+\infty}\zeta_\parallel(u_1,v_1)$$
$$\times\exp\left\{-i2\pi\left[u_1\left(\frac{u_3}{\lambda f_{ob}}\right)+v_1\left(\frac{v_2}{\lambda f_{ob}}\right)\right]\right\}\mathrm{d}u_1\,\mathrm{d}v_1, \tag{11}$$

where:

$$\zeta_\perp(u_1,v_1)=A_0\exp(ikn_\perp t)\exp\left(\frac{-ik(u_1^2+v_1^2)}{2f_\perp}\right),$$
$$\zeta_\parallel(u_1,v_1)=A_0\exp(ikn_\parallel t)\exp\left(\frac{-ik(u_1^2+v_1^2)}{2f_\parallel}\right). \tag{12}$$

Here t is the fiber diameter and A_0 is the amplitude of the wave. When the integrals are calculated, Eqs. (10) and (11) become:

$$\zeta_\perp(u_3,v_3)=\frac{A_0 f_\perp}{f_{ob}}\exp\left\{i\left[kn_\perp t-\frac{k(u_3^2+v_3^2)}{2f_{ob}^2}(f_\perp+f_{ob}-s_1)\right]\right\},$$
$$\zeta_\parallel(u_3,v_3)=\frac{A_0 f_\parallel}{f_{ob}}\exp\left\{i\left[kn_\parallel t-\frac{k(u_3^2+v_3^2)}{2f_{ob}^2}(f_\parallel+f_{ob}-s_1)\right]\right\}. \tag{13}$$

The birefringent fiber is placed diagonally between two crossed polarizers, and the output wave field can be expressed as a difference of the input wavefronts

$$\zeta = \zeta_{\perp}(u_3, v_3) - \zeta_{\parallel}(u_3, v_3). \tag{14}$$

The resultant intensity distribution at the Fourier transform plane will be

$$I = \zeta \cdot \zeta^* = \frac{I_0}{f_{ob}^2}\left\{f_{\parallel}^2 + f_{\perp}^2 - 2f_{\parallel} f_{\perp} \cos\left[\frac{\pi\rho^2}{\lambda f_{ob}^2}(f_{\perp} - f_{\parallel}) - \frac{2\pi t}{\lambda}(n_{\parallel} - n_{\perp})\right]\right\} \tag{15}$$

where $\rho = (u^2 + v^2)^{1/2}$ is the radial coordinate. This equation gives the relationship between the light intensity and the light wavelength of the Fourier transform pattern. Because the most interesting is the term under cosine function, it is possible to neglect the intensity difference between interfering waves which leads to a simpler form, *i.e.*

$$I = \zeta \cdot \zeta^* = I_0\left\{\sin^2\left[\frac{\pi\rho^2}{2\lambda \cdot f_{ob}^2}\Delta f - \frac{\pi t}{\lambda}(n_{\parallel} - n_{\perp})\right]\right\} \tag{16}$$

where $\Delta f = f_{\perp} - f_{\parallel}$.

The minimum light intensity occurs when phase difference along the fibre diameter is given by

$$\left[\frac{\pi\rho^2}{2\lambda f_{ob}^2}\Delta f - \frac{\pi t}{\lambda}(n_{\parallel} - n_{\perp})\right] = m\pi, \tag{17}$$

which immediately leads to the equation

$$\rho^2 = 2\frac{f_{ob}^2}{\Delta f}[t(n_{\parallel} - n_{\perp}) + m\lambda]. \tag{18}$$

The light intensity distribution at the center of axially-symmetrical optical Fourier transform pattern ($\rho = 0$) is given by

$$I_{\rho=0} = \zeta \cdot \zeta^* = \frac{I_0}{f_{ob}^2}\left\{f_{\perp}^2 + f_{\parallel}^2 - 2f_{\perp} f_{\parallel} \cos\left[-\frac{2\pi t}{\lambda}(n_{\parallel} - n_{\perp})\right]\right\}. \tag{19}$$

In particular, the interference patterns with a dark central patch are produced when the phase difference along the fiber diameter is given by

$$\frac{2\pi t}{\lambda}(n_{\parallel} - n_{\perp}) = 2m\pi. \tag{20a}$$

Then the optical path difference δ can be derived as

$$\delta = t(n_{\parallel} - n_{\perp}) = m\lambda. \tag{20b}$$

Using the VAWI technique we can determine the spectral dispersion of the fiber birefringence over the whole visible spectrum which is described in Subsec. 2.5.

2.4. Fourier transform observation setup

It is a characteristic feature of the polarizing microscope that we can look not only into its image plane but also into the exit pupil of the objective. The schematic

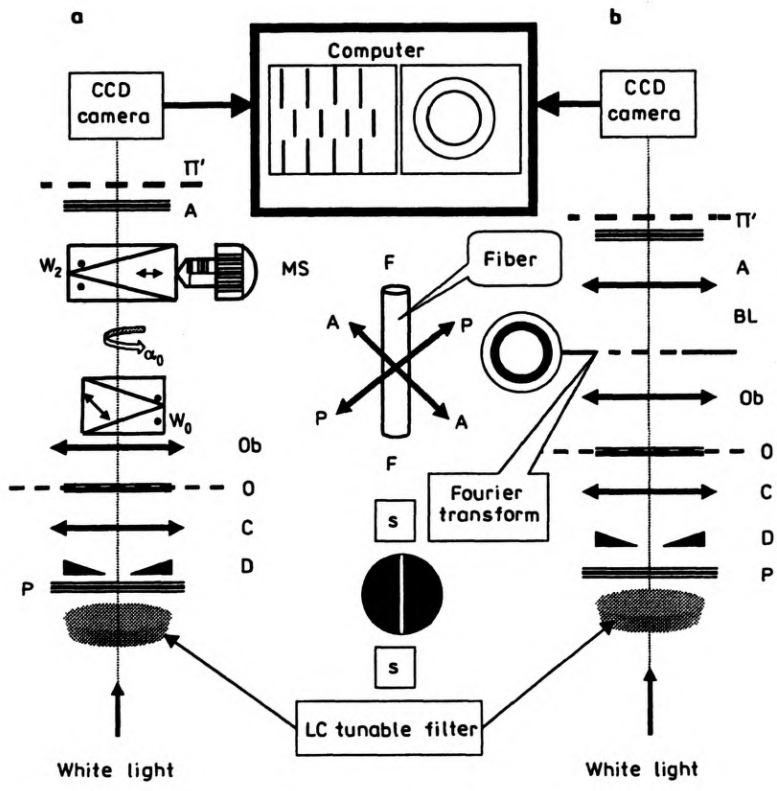

Fig. 3. Schematic diagram of the experimental system: **a** — Pluta's double-refracting interference system, **b** — microscope system used for observation and processing of the optical Fourier transform of the birefringent fibers. P — polariser, D — slit diaphragm, C — condenser, Π — object plane, W_0, W_2 — birefringent prisms, MS — micrometer screw, A — analyzer, BL — Bertrand lens, Π' — image plane

diagram of the computer-aided interference microscope for observing OFT pattern is shown in Fig. 3**b**. The double-refracting Wollaston prism is not used for the OFTobservation, but serves as an auxiliary tool of measuring the light wavelength λ. But in our experimental system, the wavelength is controlled by a tunable Lyot filter.

The polarizing microscope configured to OFT observation consists of the following elements: a polarizer, subcondenser slit diaphragm, objective 40× (N.A. 0.65 and 0.95), analyzer, Bertrand lens, and ocular. The Bertrand lens is normally used, together with the ocular, for the observation of conoscopic images of birefringent objects. It transfers the exit pupil of the microscope objective into the primary image plane where the field diaphragm of the ocular is placed. In the present paper, this lens is used either for visual observation of the optical Fourier transforms of birefringent fiber or for grabbing the image by the CCD camera. In the latter case, the camera is equipped with the standard 12 mm camera lens.

The orientation of the condenser slit, polarizer, and analyzer with respect to the birefringent fiber is shown in Fig. 3**b**, where:

– PP and AA denote the directions of light vibration in polarizer P and analyzer A, respectively,

– FF is the direction of the fiber axis,

– SS is the direction of the condenser slit diaphragm D.

As it can be seen, the polarizer P and analyzer A are crossed and their directions of light vibration form an angle of 45° with the fiber axis. The slit S is oriented parallelly to the fiber axis. The diffraction pattern of the output field of the microscope is captured by a CCD camera for its further automatic processing and analysing by the computer-aided system.

A plane linearly polarized wave of monochromatic light leaves the condenser C and passes through the birefringent object O. Because of birefringence nature of the object two spherical waves are produced. They are polarized at right angle, whose radii of curvature are slightly different. When passing the analyzer A, both wavefronts interfere with each other producing an annular or circular interference pattern in the exit pupil of the microscope objective Ob.

2.5. General principle of VAWI method

The main aim of interferometry of any kind is to determine the interference orders of the image of the object under study. During the last 10 years, this aim has been simplified significantly by Pluta. He created the VAWI family now well known as VAWI-1, VAWI-2 and VAWI-3 techniques [6]. These methods are based on using monochromatic light with continuously variable wavelength.

2.5.1. VAWI-1 technique

As shown in Figure 3a, this technique is suitable for studying objects which produce optical path difference δ greater than several wavelengths. Their specific feature manifests itself in the fact that the interfringe spacing b is the only parameter measured directly, while other quantities are observed, read out from the calibration plot $b(\lambda)$, and derived from quite a simple formula. Assuming that a fringe interference field is produced by superposition of two plane wavefronts inclined to each other at a small angle ε, the optical path difference δ between the wavefronts is given by

$$\delta = m\lambda = (m_1 + q)\lambda \tag{21}$$

where $m = m_1 + q$ is the current interference order, m_1 is a suitable integer number selected, which will be called the initial interference order, q is the increment or decrement of the current interference order m with respect to m_1.

Let a birefringent object be placed in the object plane of the transmitted-light interferometer and the fringes appear in the field of view of the interferometer due to interference between two rays passing through the medium and the object under study. This technique consists in a selection of such particular wavelength $\lambda_s = \lambda_1 > \lambda_2 > \lambda_3 > \ldots \lambda_s$, at which interference fringes displaced by an object under study become consecutively coincident and anticoincident with the reference (undisplaced) fringes; thus, the interference order increments $q_s = 0, 0.5, 1 \ldots$ are

observed. The optical path difference for λ_1 along the fiber diameter is given by

$$\delta_1 = (n_\parallel - n_\perp)_1 t = B_1 t = m_1 \lambda_1. \tag{22}$$

If the light wavelength is continuously varied, the optical path difference is given in general form as

$$\delta_s = (n_\parallel - n_\perp)_s t = B_s t = m_s \lambda_s \tag{23}$$

where $s = 2, 3, 4 \ldots$. From Eqs. (22) and (23) it follows that

$$m_1 = q_s \frac{\lambda_s}{B_{s1}\lambda_1 - \lambda_s} \tag{24}$$

and

$$B_{s1} = \frac{(n_\parallel - f_\perp)_s}{(n_\parallel - n_\perp)_1} = \frac{B_s}{B_1}. \tag{25}$$

If the fiber does not suffer from the spectral dispersion of birefringence, the coefficient $B_{s1} \simeq 1$ and Eq. (24) becomes

$$m_1 = q_s \frac{\lambda_s}{\lambda_1 - \lambda_s}. \tag{26}$$

The above formula shows that the optical path difference δ is independent of wavelength and we speak of the object-adapted variable-wavelength interferometry. Interferometry of this kind will be denoted as AVAWI(λ)-1. On the other hand, if the coefficient B_{is} is not exactly equal to unit, we speak of the quasi-object-adaptive variable wavelength interferometry. Interferometry of this kind will be denoted as QAVAWI(λ)-1.

There is a stringent and constant relation between the interfringe spacing b and the value of the wavelength λ. The simple relation expresses this variation

$$\varepsilon b = \lambda \tag{27}$$

where ε is the angle between two interference wavefronts which is given by

$$\varepsilon = 2(n_e - n_o)\tan(\alpha) = 2D\tan(\alpha). \tag{28}$$

In Equation (28), α denotes the apex angle of the main Wollaston prism, $D = n_e - n_o$ is the birefringence of a double-refracting crystal the Wollaston prism is made of, and n_e and n_o are the extraordinary and ordinary refractive indices of the crystal, respectively. If the wavelengths λ_1 and λ_s are replaced by $\varepsilon_1 b_1$ and $\varepsilon_s b_s$, respectively, the spacing between the interference fringes is measured by rotating the micrometer screw (called phase screw), which is associated with the transversal displacement of the birefringent prism No. 2 in the head of the microscope. The formula (24) may be rewritten in the form

$$m_1 = q_s \frac{b_s}{B_{s1} D_{1s} b_1 - b_s}, \tag{29a}$$

or

$$m_1 = q_s \frac{b_s}{B_{s1}\varepsilon_{1s} b_1 - b_s}. \tag{29b}$$

In Equation (29b), the coefficient $\varepsilon_{1s} = \varepsilon_1/\varepsilon_s$ expresses the spectral dispersion of the intersection angle ε, while the coefficient $D_{1s} = D_1/D_s = (n_e - n_o)_1/(n_e - n_o)_s$ expresses the spectral dispersion of the birefringence of the Wollaston prism. If $B_{s1}\varepsilon_{1s} \simeq 1$, or $B_{s1}D_{1s} \simeq 1$ we can also speak of the AVAWI method, but now the object-adaptive variable wavelength interferometry is suitable for the domain of interfringe spacing. Adaptive interferometry of this kind will be denoted as AVAWI(*b*)-1. The assumption mentioned above makes it possible to rewrite Eq. (29) as follows:

$$m_1 = q_s \frac{b_1}{b_1 - b_s}. \tag{30}$$

In general, when air surrounds the fiber, the coefficients $D_{1s} \leqslant 1$ and $B_{s1} \geqslant 1$. It is therefore self-evident that condition $B_{s1}\varepsilon_{1s} \simeq 1$, or $B_{s1}D_{1s} \simeq 1$ is more practical than condition $B_{s1} \simeq 1$. Consequently, the AVAWI(*b*)-1 method is considered more interesting than the AVAWI(λ)-1. The main advantage offered by the variable wavelength interferometry technique is that it allows us to identify the interference order when the object under study deflects the interference fringes. The quick measurement of the optical path differences within the whole visible spectrum is another advantage of the variable wavelength interferometry technique.

2.5.2. VAWI-1 technique adapted to OFT of birefringent fibers

PLUTA [8] was the first who applied the optical Fourier transforms to the measurement the spectral dispersion of the birefringence of the textile fibers. This measurement has been done manually and now we propose a computer-aided technique.

Let a cylindrical birefringent fiber be placed in the object plane of the microscope (Fig. 3b). Because of birefringence nature of this fiber two focal lines $L_{||}$ and $L_{\perp}$ are separated from each other by a significant distance greater than λ (Fig. 1). An annular or circular dark fringe appears in the exit pupil of the microscope objective. This pattern is recorded with a CCD camera and processed by an automatic system.

In the paper presented, a new procedure is used to measure the initial interference order against the relation between the radius of the annular dark fringe of the OFT pattern and the wavelength. Starting from the long-wavelength region of the Lyot filter and passing continuously toward the short-wavelength region one can observe a sequence of the interference patterns consisting of annular fringes of consecutive orders. When the dark fringe appears as a circular patch at the center of the objective exit pupil, the radius of this fringe increases with decreasing wavelength, and finally the annular fringe reaches the edge of the objective exit pupil. Subsequent decreasing the wavelength repeats the above sequence of interference patterns. The number of these sequences depends on the birefringence of the fiber.

In this paper, it is not necessary to select a certain particular wavelength $\lambda_s = \lambda_1 > \lambda_2 > \ldots \lambda_N$, for which an annular dark fringe becomes consecutively

maximum bright and dark in its center. The fiber birefringence can be calculated from the relation between the wavelength of monochromatic light and the radius ρ of the annular dark fringe for each sequence of interference patterns. When at least two fringes are visible simultaneously their radii can be measured. The radii ρ_{s1} and ρ_{s2} (see Eq. (18)) take the forms:

$$\rho_{s1}^2 = 2\frac{f_{ob}^2}{\Delta f_s}[tB_s + m_1\lambda_s]$$

and (31)

$$\rho_{s2}^2 = 2\frac{f_{ob}^2}{\Delta f_s}[tB_s + (m_1 + q_s)\lambda_s] .$$

where $s = 1, 2, 3 \ldots$ and q_s is the increment or decrement of interference order ($q_s = \pm 1$). When the above formulas are divided by each other, the birefringence of the fiber is given by

$$B_s = \frac{m_1\lambda_s(1-A) - Aq_s\lambda_s}{t(1-A)} \tag{32}$$

where $A = (\rho_{s1}/\rho_{s2})^2$, and the spectral dispersion of the fiber birefringence can be calculated from Eq. (32).

2.6. Description of automatic measurement procedure

The digital image processing technique is used to analyze the interferogram shown in Fig. 3b. At the beginning of the measurement the OFT pattern is adjusted so that the displacement of the fringe center with respect to the frame center is smaller than the radius of the fringe ρ. The initial radius ρ_{01} should be as large as possible provided that it does not touch the edge of the exit pupil of the microscope objective. These manipulations, at the beginning of the measurements, speed up the process of the following automatic operation which extracts the parameters of the fringe shape (compare Fig. 4).

Sometimes the annular dark fringe is deformed and takes elliptical shape because the condenser slit and the fiber axis are not parallel or the fiber suffers from local optical inhomogeneities or geometrical irregularities. In this case, the ellipse fitting is applied to the pattern and then the ellipse parameters are calculated (step G in Fig. 4). The above procedures, except an initial stage, must be applied each time when the wavelength is changed using the Lyot tunable birefringent filter, otherwise the fiber under study is translated along its axis.

3. Irregularities of the optical Fourier transforms

The aim of this study is to detect the irregularity of the optical Fourier transform pattern when the cylindrical birefringent fiber is translated at right angle to the optical axis of the system. The experimental work has been carried out for many samples of different cylindrical birefringent fibres. It has been observed that:

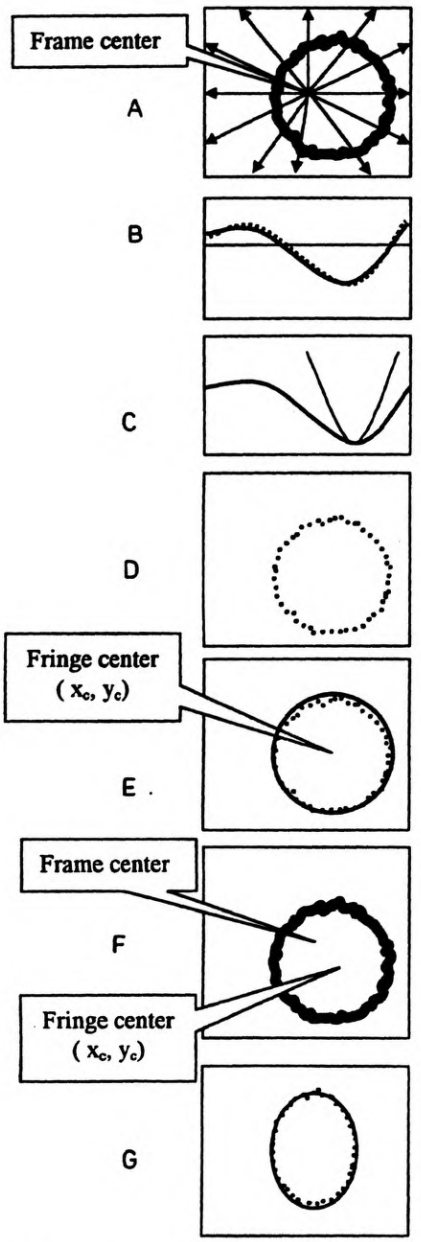

Initial stage starts from radial scanning of the frame; each radial vector which begins at the frame center and ends at the frame edge is taken out from the image for analysis.

The radial vector is smoothed using averaging or median filter (optional).

The minimum of the vector is found by fitting a parabola.

The fringe shape is then defined by using the above procedure for each radial vector.

The center of the fringe is calculated by fitting a circle to the dotted pattern.

The process repeats from the very beginning (stage A) but the angular distance between the vectors is diminished to increase precision. If the difference between the center of the frame and the center of the fringe is significant then radial vectors start from the new fringe center.

Having found the coordinates of the center the ellipse is fitted to the pattern and further ellipse specific parameters are calculated. The above procedure, except initial stage, must be applied each time the wavelength is changed or a fiber under study is translated along its axis.

Fig. 4. Schematic diagram of the main procedures of the image processing system

1. The diameter of the annular dark fringe changes occasionally when the fiber under study is translated along its axis. Since the diameter of the dark fringe neither depends on the wavelength nor on the fiber thickness it means that the thickness of this fiber is not stable along its axis (manufacturing defect).

2. The shape of the dark fringe takes an elliptical shape due to the bending of the fiber. The ellipticity of the dark fringe neither depends on the tilt of the wavefronts (the angle between the condenser slit and the fiber axis is not equal to zero) nor on the degree of bending.

3. The irregularities around concentric circular dark fringe originate from the residual roughness of the spherical cylindrical shape of the birefringent fibers.

4. The complete deformation of the dark fringe (unknown dark fringe shape) may be caused by twisting or breakage of the fiber. The irregularity does not depend on small defocusing of the specimen under study.

4. Examples of experimental results

The spectral dispersion of birefringence of exemplary textile fibers has been determined for the sake of comparison using the fringe field interference method (VAWI-1 technique) [3] and optical Fourier transform method. The radius ρ of the pattern has precisely been measured for given wavelengths and then interference orders and the fiber birefringence have been calculated according to the technique discussed previously. Figure 5 displays a comparison of the spectral dispersion of birefringence of the fiber obtained using the optical Fourier transform technique and the fringe field method when the fiber is surrounded by air and liquid. It is seen that the results obtained using the OFT technique and

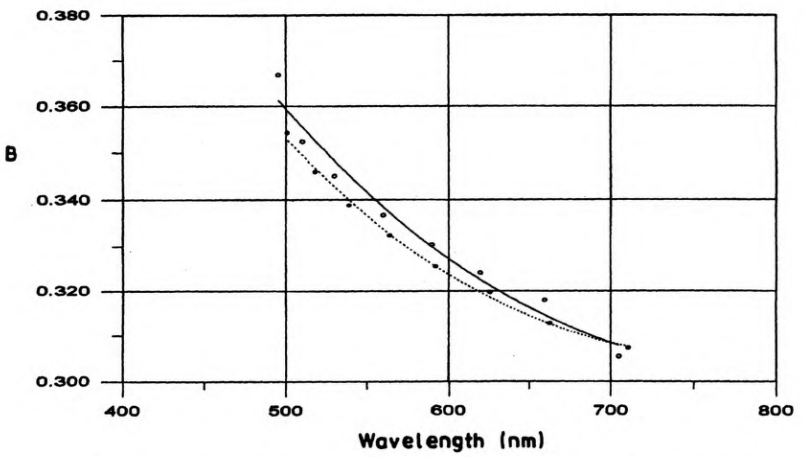

Fig. 5. Spectral dispersion birefringence of the highly-oriented fiber obtained using OFT technique (unfilled circles) and the fringe field method when the fiber is surrounded by liquid (filled circles)

fringe field method (fiber is surrounded by liquid) agree approximately with each other. Using immersion liquid it is possible to avoid any confusion with identification of interference orders (if the fringe displacement is smaller than the interfringe spacing).

5. Conclusions

Fringe field interference method and optical Fourier transform technique have been tested. Using these techniques the spectral dispersion of birefringence of the polymeric fibers has been measured.

The concept of the VAWI technique has been found particularly useful when the OFT pattern is processed with computer-controlled automatic analysis system.

The optical Fourier transform pattern observed in a polarizing interference microscope has been processed automatically to measure the radii of the dark fringes as a function of the wavelength. The advantage of the method presented is that the evaluation is simple, the processing time is short, and the results are satisfactorily precise compared with the classical methods. Using the OFT method we avoid confusion arising from identification of the interference orders when the highly birefringent fiber under study is surrounded by air. This method does not require immersing highly birefringent fibers in liquids, which is usually necessary in conventional microinterferometry of textile fibers.

It is not necessary to follow Pluta's method in order to analyze the Fourier transform pattern only in its center. A new procedure is used to measure the interference order against the relation between the radius of the annular dark fringe and the wavelength for each sequence of interference patterns.

In comparison to the conventional fringe field interference method used for measuring the fiber birefringence $B = (n_{\parallel} - n_{\perp})$, the optical Fourier trnsform method is more precise. The latter allows us to detect and assess rapidly the optical and geometrical microdefects of the cylindrical birefringent fibers. The only disadvantage is that the method does not allow us to measure separately the refractive indices $n_{\parallel}$ and $n_{\perp}$.

Acknowledgements — The authors are grateful to Professor Maksymilian Pluta for the suggestions and discussion of this paper as well as for a number of essential and technical corrections in the manuscript.

References

[1] PLUTA M., J. Opt. Soc. Am. A **4** (1987), 2107.
[2] PLUTA M., Opt. Eng. **31** (1992), 402.
[3] PLUTA M., J. Microscopy **149** (1988), 97.
[4] PLUTA M., Opt. Laser Technol. **19** (1988), 131.
[5] PLUTA M., Opt. Laser Technol. **20** (1988), 81.
[6] PLUTA M., *Advanced Light Microscopy*, Vol. 3, Elsevier, Amsterdam 1993, pp. 370–389.
[7] PLUTA M., *Fourier transforms of a birefringent fiber and their practical applications*, Einladung und Program zur Tagung: *Optik und Feinmechanik der DgaO* (Wetzlar: DGaO), 1981, p. 36.
[8] PLUTA M., J. Modern Opt. **34** (1987), 1451.
[9] CATHEY W. T., *Optical Information Processing and Holography*, Wiley, New York 1974, pp. 96–109.

Received July 22, 1998